Characteristic Ocular Features in Cases of Autosomal Recessive PROM1 Cone-Rod Dystrophy

Frederick T. Collison,[1] Gerald A. Fishman,[1,2] Takayuki Nagasaki,[3] Jana Zernant,[3] J. Jason McAnany,[2] Jason C. Park,[2] and Rando Allikmets[3,4]

[1]The Pangere Center for Inherited Retinal Diseases, The Chicago Lighthouse, Chicago, Illinois, United States
[2]Department of Ophthalmology and Visual Sciences, The University of Illinois at Chicago, Chicago, Illinois, United States
[3]Department of Ophthalmology, Columbia University, New York, New York, United States
[4]Department of Pathology and Cell Biology, Columbia University, New York, New York, United States

Correspondence: Gerald A. Fishman, The Pangere Center for Inherited Retinal Diseases, The Chicago Lighthouse, 1850 West Roosevelt Road, Chicago, IL 60608, USA; gerafish@uic.edu.

Submitted: March 1, 2019
Accepted: April 26, 2019

Citation: Collison FT, Fishman GA, Nagasaki T, et al. Characteristic ocular features in cases of autosomal recessive PROM1 cone-rod dystrophy. *Invest Ophthalmol Vis Sci*. 2019;60:2347–2356. https://doi.org/10.1167/iovs.19-26993

Purpose. To define characteristic ocular features in a group of patients with autosomal recessive (AR) *PROM1* cone-rod dystrophy (CRD).

Methods. Three males and one female from three unrelated families were first seen at the ages of 15 to 22 years and diagnosed with CRD. Clinical testing available for review included full-field electroretinogram (ERG) in three patients, as well as near-infrared autofluorescence (NIR-AF), spectral-domain optical coherence tomography (SD-OCT), and color fundus photography in all four patients. Whole exome sequencing (WES) was performed on all cases, and whole genome sequencing (WGS) was performed in two families.

Results. WES found compound heterozygous *PROM1* variants in one isolated male, plus heterozygous variants in the remaining patients. WGS uncovered deleterious *PROM1* variants in these two families. ERG showed markedly reduced cone-isolated amplitudes and variably reduced rod-isolated amplitudes. The dark-adapted combined rod and cone responses demonstrated notably reduced a-wave amplitudes and moderately reduced b-waves, and the resultant waveform resembled the normal rod-isolated response. On fundus examination, oval-shaped macular lesions were observed, as were several small, circular hypoautofluorescent lesions within the posterior pole on NIR-AF. Three patients showed extramacular circular atrophic lesions.

Conclusions. The autofluorescence changes, peripheral retinal abnormalities, and ERG findings have not been emphasized in previous reports of AR *PROM1*, but they became a recognizable phenotype in this cohort of patients. A similar constellation of findings may be observed in CRD due to *CDHR1,* a functionally related gene. The pattern of abnormalities reported herein may help to focus genetic screening in patients with these findings.

Keywords: cone-rod dystrophy, electroretinogram, fundus autofluorescence, *PROM1*, *CDHR1*, *PCDH21*

Autosomal recessive (AR) *PROM1* retinal dystrophy was first reported in a family with an "early-onset severe form of retinal degeneration."[1] Later reports demonstrated that AR *PROM1* can be associated with an early (childhood) onset of retinal dystrophy that manifests as either cone-rod dystrophy (CRD)[2–4] or retinitis pigmentosa (RP) phenotypes with prominent macular involvement.[5,6] Severe visual loss and a nondetectable full-field ERG, either by or within the third decade of life, are common in AR *PROM1* cases, independent of whether the diagnosis is CRD or RP.[1,3,5–7]

PROM1 (OMIM 612657) codes for a transmembrane glycoprotein (Prominin-1) that localizes to the base of the rod and cone outer segments and is involved in disc assembly and maintenance of outer segment structure.[8] *PROM1* is associated with both autosomal dominant (AD)[9,10] and AR[1] retinal dystrophies, with the AD forms tending to be later onset and milder.[10] *PROM1* is responsible for between 1.0% and 9.5% of AR CRD (arCRD) cases.[7,11,12]

Few identifiable findings in AR *PROM1* patients have been reported. One report found that the combination of high myopia, nystagmus, and early-onset CRD is suggestive of AR *PROM1*.[3] In this report we demonstrate four cases of *PROM1*-associated arCRD that showed identifiable macular and peripheral retinal, as well as full-field ERG findings.

Patients and Methods

Patients

Four patients from three families were diagnosed with CRD by one of the authors (GAF). Informed consent was obtained from each of the four patients, as well as from participating unaffected parents and siblings. Procedures adhered to the tenets of the Declaration of Helsinki, and the protocol was approved by the Western Institutional Review Board (IRB) and Columbia University IRB.

Genetic Analysis

Thirty-nine patients (from 34 families) with CRD were initially tested for mutations in the *ABCA4* gene by direct sequencing. In 13 of these cases, two disease-associated *ABCA4* variants

Table 1. *PROM1* Variants in Affected CRD Patients

	PROM1 Variant	Amino Acid Change	Ethnicity/Nationality	Citation
Patient 1 (Family A)	c.1157T>A	p.Leu386*	Syrian-Lebanese Christian (paternal)	Beryozkin et al. 2014[15]
	c.1557C>A	p.Tyr519*	Bohemian/Scotch-Irish/Greek (maternal)	Song et al. 2011[16]; Carss et al. 2017[17]
Patient 2 (Family B)	c.1182_1202del	p.Asn395_Pro401del	Polish (paternal)	Novel
	chr4:16017462_16024802del (7340 bp del, including 2 exons)	del of 2 exons	Polish (maternal)	Novel
Patient 3 (Family B)	c.1182_1202del	p.Asn395_Pro401del	Polish (paternal)	Novel
	chr4:16017462_16024802del (7340 bp del, including 2 exons)	del of 2 exons	Polish (maternal)	Novel
Patient 4 (Family C)	c.1274+2T>C	Affects splicing	Scottish/English/German (maternal)	Novel
	c.2077-521A>G	Affects splicing	German/English/Polish (paternal)	Mayer et al. 2016[18]

were found, whereas *ABCA4* testing was negative in all four cases that are the focus of this study. Based on the availability of unaffected relatives to aid in analysis, eight CRD cases (either with no detected *ABCA4* or one *ABCA4* variant) were subjected to whole exome sequencing (WES) at Macrogen, Inc. (Seoul, South Korea), using the Agilent (Santa Clara, CA, USA) SureSelect V5 capture kit and Illumina (San Diego, CA, USA) HiSeq 4000. Resulting sequences were analyzed with BWA-MEM, Picard, GATK, and SnpEff tools. The average sequence depth of target regions was 100x resulting, on average, in identification of approximately 90,000 single nucleotide polymorphisms. These variants were filtered based on minor allele frequency (>0.0001) and with in silico prediction programs (PolyPhen2, REVEL, CADD). Possibly pathogenic variants were confirmed by Sanger sequencing and segregation with the disease in families. WES identified two compound heterozygous stop-gain variants of the *PROM1* gene in patient 1 (family A; Table 1, Fig. 1) and segregation of these with the disease was confirmed in family A (including both parents and an unaffected sibling). One possibly pathogenic *PROM1* variant was found in each of the remaining patients. The remaining four CRD patients who underwent WES either remain unsolved, or their phenotype was attributed to a gene other than *PROM1*. DNA of patients 2, 3, and 4 (families B and C; Fig. 1) were subjected to whole genome sequencing (WGS) at Macrogen, Inc., using Illumina TruSeq PCR-free library kit and 150 base pair (bp) paired-end sequencing on NovaSeq 6000 (Illumina) with approximately 30x depth. Deleterious deep intronic mutations were found by WGS in each of the remaining families, which segregated with the disease (Table 1, Fig. 1). The available clinical histories, chart notes, imaging, and ERG findings of each patient were retrospectively reviewed for this study.

Imaging

Color fundus photography was performed using a Canon CR-1 Mark II camera (Canon USA, Melville, NY, USA). Spectral-domain optical coherence tomography (SD-OCT), infrared reflectance scanning laser ophthalmoscopy (IR-SLO), near-infrared autofluorescence (NIR-AF), and short-wavelength autofluorescence (SW-AF) images were obtained using the Heidelberg Spectralis HRA+OCT (Heidelberg Engineering, Heidelberg, Germany).

Full-field ERG

Review of the prior ophthalmic records of patient 1 showed that he had undergone a full-field ERG at an outside clinic with an LKC Technologies UTAS-E 2000 unit (LKC Technologies, Gaithersburg, MD). Patient 4 had also undergone a full-field ERG at another outside clinic. In two cases (patient 2 and patient 4), a clinical full-field ERG was obtained on a Nicolet Viking IV system (Nicolet Biomedical Inc, Madison, WI, USA), under previously described conditions.[13,14] The recording electrode was a unipolar Burian-Allen contact lens electrode. Dark-adapted ERG stimuli included a rod-isolated short-wavelength stimulus of 0.005 (photopic) cd·s·m^{-2} and a rod and cone combined response to a white single-flash stimulus of 4.65 cd·s·m^{-2}. Light-adapted ERG conditions, tested on a 15.4 cd·s·m^{-2} white background, included a white single-flash stimulus of 4.65 cd·s·m^{-2} and a 32-Hz flicker stimulus. Control ranges for amplitudes and implicit times were obtained from more than 50 normally sighted subjects with an age range of 24 to 38 years.

Results

Genetic Analysis

Pedigrees for the three families are shown in Figure 1, and *PROM1* mutations are listed in Table 1. For patient 1, WES found two *PROM1* stop-gain variants in compound heterozygosity. Both mutations have been described before as causal in arCRD.[15–17] In patients 2 and 3 (the brothers in family B), WES found one new, possibly pathogenic, *PROM1* variant, which deletes seven amino acids (p.Asn395_Pro401del). In patient 4 (family C), WES detected a single, predicted pathogenic, *PROM1* variant, which affects splicing. Because the ERG, autofluorescence, and retinal appearance (described below) of cases in both families suggested recessive disease caused by *PROM1* mutations, the 1-mutation cases were subjected to WGS, which uncovered a large deletion removing two full exons in patient 2. This variant was subsequently verified also in his affected brother. WGS also detected a deep intronic variant in patient 4 (c.2077-521A>G), which has been described as a severe, splicing-affecting variant.[18] All four affected cases were determined to be compound heterozygous for the predicted or demonstrated pathogenic *PROM1* variants via segregation analyses in the three families (Fig. 1).

Ocular, Medical, and Family Histories

Patient 1 had been previously diagnosed with CRD at 3 years of age by an outside clinic. He felt that his central vision had never been sharp, even with correction. In his early teens, he had noted photoaversion. He felt that his night vision had always been at least mildly reduced, although he drove without difficulty at night until his late teens, when he noted worsening nyctalopia and slight loss of peripheral vision. He was first examined by one of the authors (GAF) at the age of 22. At that visit, he reported his symptoms of reduced color, central, and

Investigative Ophthalmology & Visual Science

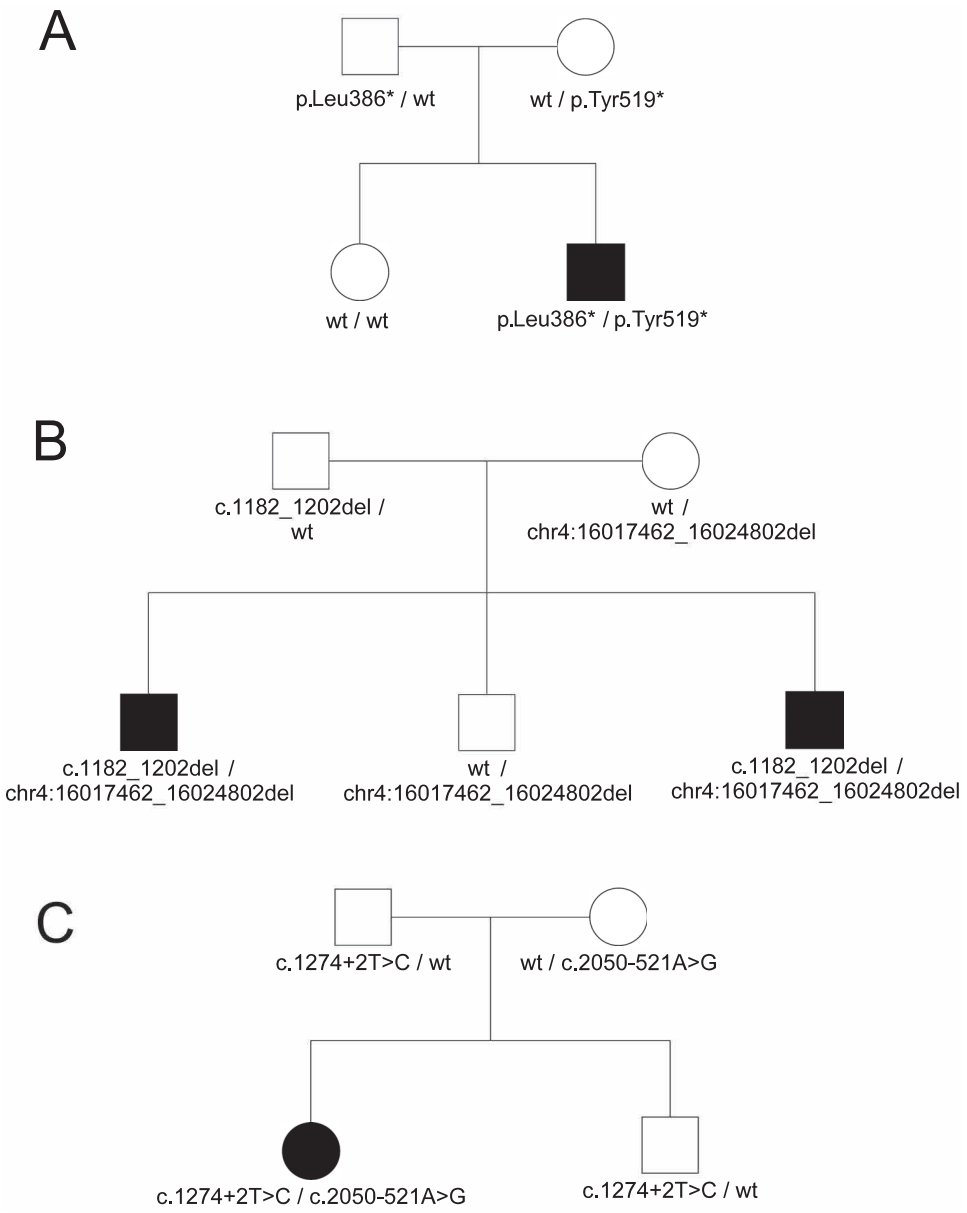

Figure 1. Pedigrees of the three families that participated in the study, with family A in (**A**), family B in (**B**), and family C in (**C**). In each of the three families, the unaffected parents were demonstrated to carry one of the two variants carried by their respective affected child/children. Segregation of variants with disease is further reinforced in each family by inclusion of one unaffected sibling, none of whom carried two disease-associated variants.

night vision had all progressed significantly within the previous year. He also noted occasional brief photopsias since childhood. Nystagmus was not noted at that visit, and it was not reported in the ocular history. Medically, the patient had diagnoses of borderline hypertension, bipolar disorder, anxiety, and hyperhidrosis, as well as a past history of a heart murmur that had resolved by the age of 12. His maternal grandfather was believed to have been color deficient, but no other family history of retinal or visual problems was noted. The patient's father was of Syrian/Lebanese Christian ancestry, and his mother was of mixed Bohemian, Scotch-Irish, and Greek ancestry.

Patients 2 and 3 (brothers from family B) were of Polish ancestry. Patient 2 had failed a school vision screening in first grade, and his acuity reportedly had never been fully correctable with spectacles. His first examination was at age 15, at which time he reported no visual complaints. Nystagmus was not noted on examination or in the ocular history. He had been referred by an outside eye doctor who found macular abnormalities. He denied any medical conditions. Patient 3 had less severe symptoms than his brother. He was first seen at age 21, at which time he reported mild color vision complaints that had begun in his mid-late teens and mild photoaversion. He denied central, peripheral or night vision complaints. Mild micronystagmus was noted on examination. His medical history was unremarkable aside from asthma.

Patient 4 was a female patient of mixed Western European ancestry who presented at age 21. Her first visual symptoms were noted at age 4 when she failed a school acuity screening. At age 21, she noted photoaversion (specifically, poor vision in bright light), which had begun in her mid-late teens, as well as poor color vision. She denied nyctalopia and peripheral vision

Investigative Ophthalmology & Visual Science

Table 2. BCVA, Refractive Error and Color Vision in AR *PROM1* CRD

	Age, y	BCVA OD	BCVA OS	Refractive Error OD	Refractive Error OS	Ishihara Color Test
Patient 1 (Family A)	22	20/40−2	20/40−1	−7.50+3.00×095	−7.75+2.75×090	0/8 OD, OS
	27	10/160−1	10/160−1	−8.50+2.75×090	−8.50+3.00×095	
Patient 2 (Family B)	15	20/30+1	20/40	−2.00+1.25×095	−1.75+1.25×080	1/15 OD, OS
	35	10/225	10/200−1	−4.75+0.75×005	−7.50+2.50×095	
Patient 3 (Family B)	21	20/40−1	20/40+1	−5.50+2.25×080	−5.25+2.50×095	1/11 OD, OS
	29	20/80−2	20/70−1	−8.00+2.75×090	−6.50+2.50×085	
Patient 4 (Family C)	21	20/100	20/100	−3.50 Sphere	−5.50+0.75×060	Test plate only OD, OS
	33	10/120+1	10/100−1	−5.50+1.00×145	−7.00+1.75×065	

complaints. Photoaversion complaints increased throughout the patient's 20s. Nystagmus was not noted either on examination or by history. By age 25 she reported slow dark adaptation. Her family history was noncontributory. She was diagnosed with bipolar disorder in her mid-20s and treated with Lamictal and Prozac; however, by age 30 she was off medication. The three unaffected relatives in family B, as well as the father in family C, each received undilated direct ophthalmoscopy, which was described as normal. The father in family A had SD-OCT of the macula available, which was normal in the right eye and showed a few small drusenoid deposits in the left eye.

Clinical Psychophysical Testing

Best corrected visual acuity (BCVA) and refractive error at the initial and most recent clinic visits are shown in Table 2. Legal blindness (worse than 20/100 BCVA in the better eye) was reached in the third decade in patients 1, 2, and 4, whereas legal blindness had not been reached as of the most recent visit (age 29) in patient 3. The four patients each failed to identify more than the control plate on the Ishihara color vision test at their respective first visits. As a group, Goldmann visual fields generally showed expanding and deepening central scotomas, as well as at least moderate constriction of the peripheral boundaries, which increased throughout the third decade.

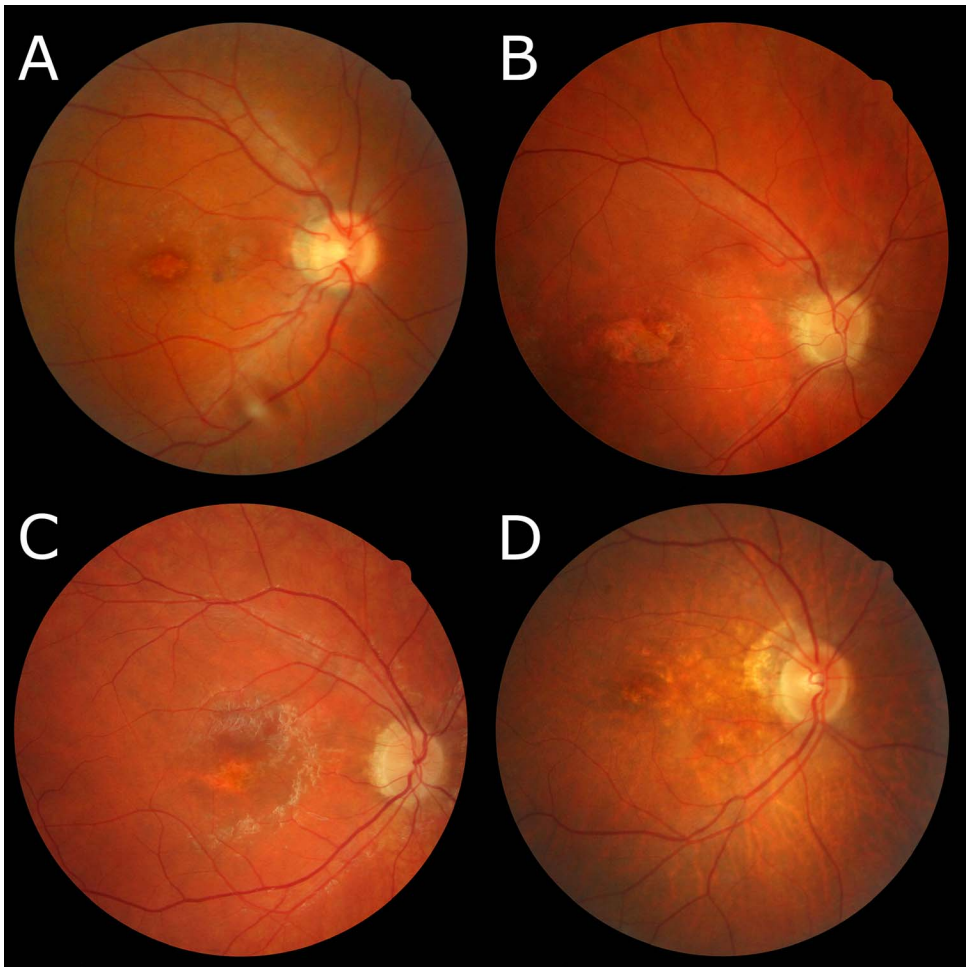

Figure 2. Color fundus photographs of the macula of the right eye in AR *PROM1* patients 1 (**A**), 2 (**B**), 3 (**C**), and 4 (**D**), taken at ages 24, 27, 22, and 29 years, respectively. Each case showed mild vascular attenuation, peripapillary atrophy, and hypopigmentation to varying degrees in the fovea. A horizontally oval margin of either hyperpigmentation or relative sparing of macular pigment was most evident in patients 1 and 2, and a few drusenoid deposits were most evident in the macula of patient 1.

Investigative Ophthalmology & Visual Science

Macular Changes

Representative macular color fundus photographs of the right eye for each patient are shown in Figure 2. Each case showed normal optic nerves, varying degrees of parapapillary atrophy, and mild vessel attenuation. Each patient had atrophic lesions in the fovea, with an oval shape that was most evident in patient 1 (Fig. 2A). Patient 1 also showed a few small drusenoid lesions outside the central hypopigmented area. The central lesion in patient 2 (Fig. 2B, age 27) was larger and more deeply atrophic, whereas patients 3 and 4 showed smaller, less well-defined areas of foveal hypopigmentation. None of these images show definite fleck-like lesions, as might be seen in Stargardt disease.

Peripheral Retinal Changes

Figure 3 shows montage color fundus photographs, which demonstrate diffuse midperipheral granularity, as well as round, well-defined atrophic lesions in the retinal periphery of patients 1, 2, and 3. The lesions varied in size from approximately one-half to two disc diameters (approximately 0.75 to 3 mm diameter). Many of the atrophic lesions also had hypertrophic pigmentary changes, most evident at the borders of the lesions. The peripheral changes were progressive in these patients, with more bone spicule–type pigment developing in patient 1 as of his most recent visit at age 27. Patient 4 was not found to have midperipheral or peripheral lesions as of her most recent dilated fundus examination at age 33.

Imaging: Autofluorescence and SD-OCT

Figure 4 shows NIR-AF at selected visits for each patient. Small, circular lesions were hypoautofluorescent (hypo-AF), on a homogeneous background in the central 30° in patients 1, 3, and 4. There was variation in the distribution of these small hypo-AF lesions, occurring either in a cluster centered on the macula, as in patient 1, or predominantly between the disc and the fovea, as in patients 3 and 4. The horizontally oval foveal lesions seen on color photos were evident on NIR-AF as well.

Figure 5 shows multimodal imaging from patient 1. On SD-OCT (Fig. 5A), this patient demonstrated identifiable, but attenuated external limiting membrane (ELM) and inner segment ellipsoid (ISe) bands in the fovea at age 22. His inner retinal lamination appeared essentially normal, as it was in the other three patients, at least on their earlier scans. Outside the foveal area there appeared to be a residual thinned outer nuclear layer and ELM, but no ISe band. The foveal ISe was no longer present on a follow-up scan at age 27, consistent with a substantial loss of acuity in that time frame. Patients 3 and 4 showed SD-OCT findings similar to the age 22 scan of patient 1. However, unlike patient 1, patient 4 had severe BCVA loss. IR-SLO imaging in patient 1 (Fig. 5B), also at age 22, showed a cluster of small, round, hyporeflective lesions in the macula. These lesions were less apparent on IR-SLO images at later visits, and they were not consistently observed in the other three patients with that modality.

Patient 1 underwent SW-AF, NIR-AF, and en face SD-OCT at age 26 (Figs. 5C–F). The NIR-AF and SW-AF were largely similar to one another. Within the macula, the two modalities were essentially indistinguishable. Outside the macula, there was a heterogeneous background and several hypo-AF lesions that had not been present during an earlier visit at age 22 (Fig. 4A). The en face SD-OCT was most similar to the AF images when measured at the level of the anterior aspect of the RPE (Figs. 5E, 5F). At this depth, en face imaging demonstrated hyporeflective foci, many of which corresponded to those seen on the AF images. In Figure 5F, it also can be seen that the inner retinal lamination had become somewhat disrupted temporal to the fovea by age 26. Patient 2 had a very similar appearance at his more recent visits, at approximately age 32, with inner retinal lamination becoming less distinct, most

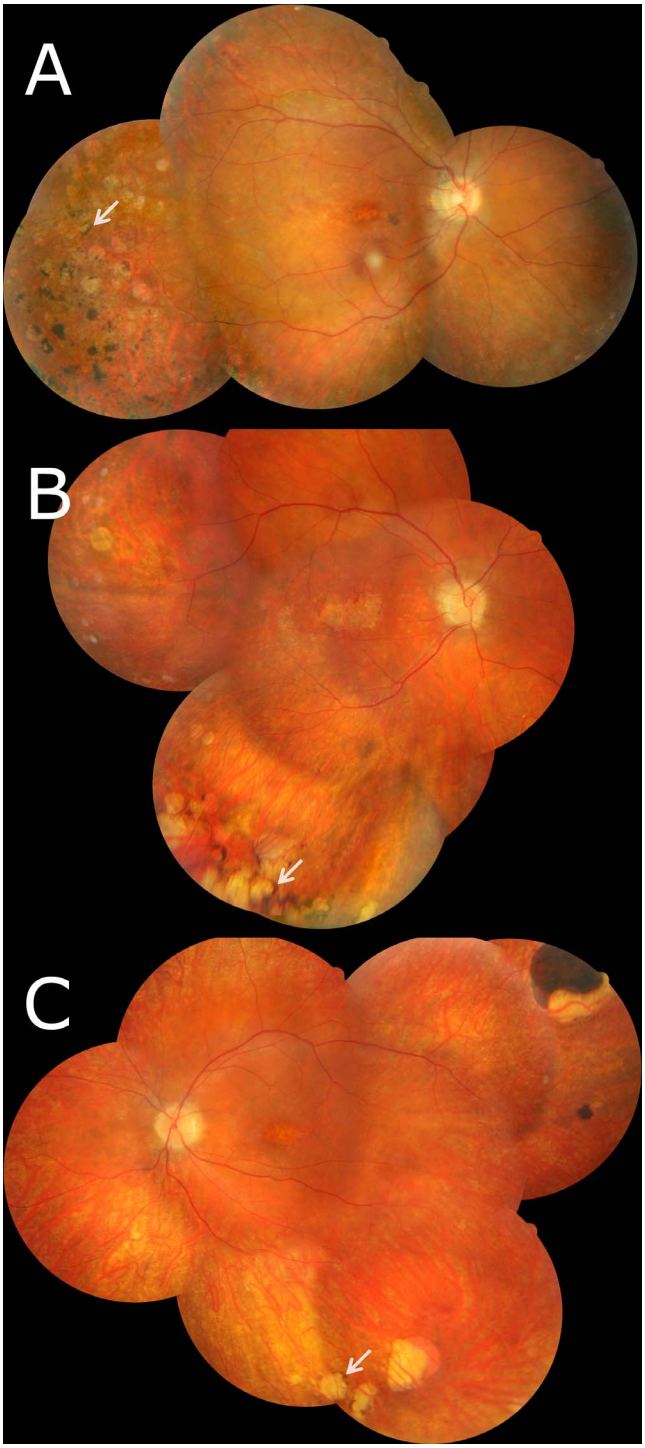

Figure 3. Montage retinal color photographs of patients 1 (**A**, right eye), 2 (**B**, right eye) and 3 (**C**, left eye), are shown at ages 26, 29, and 26, respectively. Each of these three cases demonstrated circular atrophic and hyperpigmented lesions in the mid- to far periphery. Hyperpigmentation was observed at the borders of many of the atrophic lesions (one example in each panel marked by a *white arrow*). Note expansion of the central atrophic lesion in patient 2, relative to the color fundus image from 2 years prior in Figure 2B.

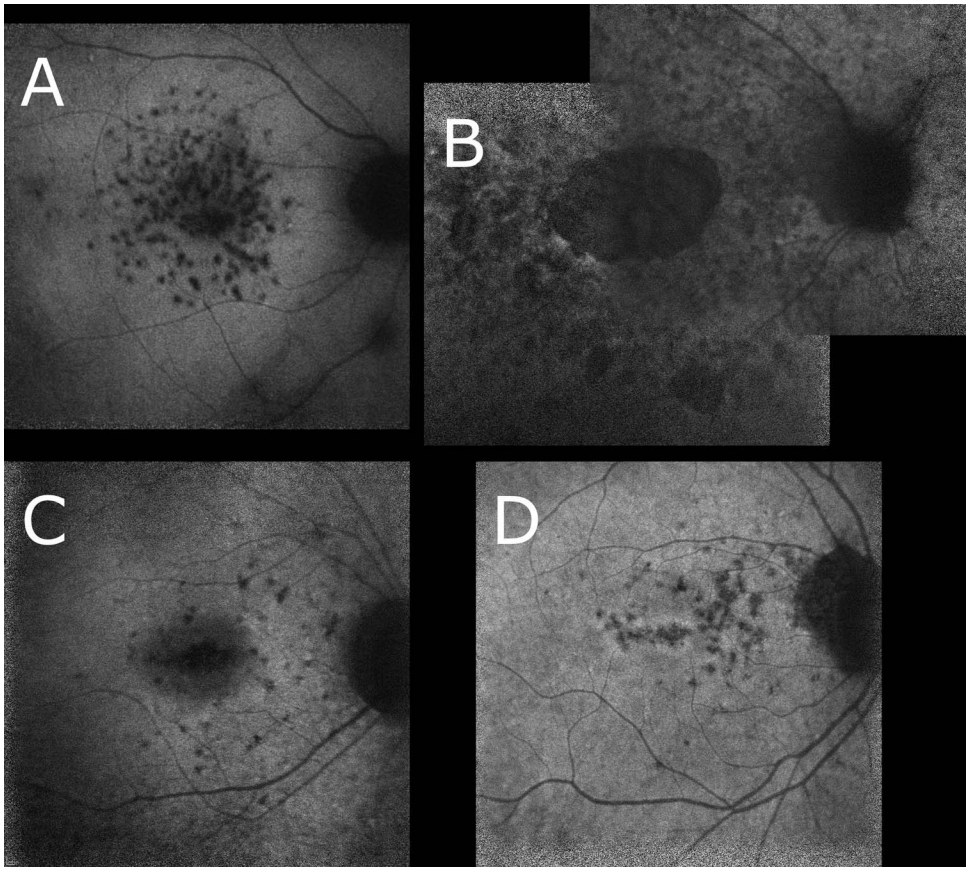

FIGURE 4. NIR-AF in the right eye in AR *PROM1* patients 1 (**A**), 2 (**B**), 3 (**C**), and 4 (**D**), taken at ages 22, 32, 28, and 29 years, respectively. Oval hypo-AF foveal lesions were evident in patients 1, 2, and 3. Small foci of hypo-AF of varying distributions throughout the macula were seen in each case. Relative to the other cases, patient 2 demonstrated confluence or enlargement of many of the hypo-AF foci, which cover not only the macula, but also the near-periphery.

evidently temporal to the fovea. Patients 3 and 4 maintained a normal inner retinal layer appearance.

Full-field ERG

Patients 1 and 4, as noted, had been tested by separate outside clinics with clinical full-field ERGs at the ages of 12 and 4, respectively (ERGs not shown). Review of the ERG from patient 1 showed nondetectable light-adapted single-flash and 30-Hz flicker responses, as well as nondetectable rod-isolated blue single-flash responses. The scotopic combined "rods and cones" single-flash (approximately 2.5 $cd{\cdot}s{\cdot}m^{-2}$) responses were subnormal, at approximately half of the reported lower limit of normal for the b-wave right and left eyes. The a-wave was minimally present in the right eye and notably reduced in the left eye. Repeat ERG by the same outside clinic at age 21 was deemed nondetectable for all stimuli. We obtained a copy of the full-field ERG findings on patient 4 that did not specifically note the stimulus parameters. Nonetheless, we were able to ascertain a minimal a-wave amplitude in proportion to the b-wave under the highest luminance scotopic single-flash stimulus condition that was used.

Patients 2 and 4 had full-field ERG performed on a Viking II system at ages 15 and 21, respectively (Fig. 6). Cone-mediated responses (Fig. 6, bottom) in both cases were essentially nondetectable, with the exception of a delayed and markedly reduced, 12-microvolt 32-Hz flicker response in patient 4. Under scotopic conditions (Fig. 6, top), the rod-isolated responses were markedly delayed and reduced in amplitude to below half the lower limit of normal. The scotopic combined (rod and cone) single-flash response demonstrated a markedly reduced a-wave (10%–15% of normal), as well as markedly delayed b-waves that were approximately one-third (patient 2) and one-half (patient 4) of the lower limit for amplitude. With the small a-waves and delayed b-waves, the combined response waveforms more closely resembled a control's rod-isolated response than a combined response. The b/a amplitude ratio was 3.7 and 5.7, respectively, which compares to a control range of 1.25 to 2.2.

DISCUSSION

In this report, we described four cases of arCRD caused by mutations in *PROM1* from three families who showed identifiable macular findings on multiple modes of retinal imaging. All four patients demonstrated oval foveal lesions, as well as small hypo-AF foci in the posterior pole on NIR-AF imaging. Three of the cases demonstrated peripheral circular lesions as well. One patient from each of the three families demonstrated an ERG phenotype in which the dark-adapted combined response had a very small a-wave and delayed b-wave.

All *PROM1* variants reported in this study are predicted or were shown to be deleterious, including two variants resulting in premature stop codons; one small 21-bp deletion; one large genomic deletion, resulting in a loss of two full exons; one variant in splice consensus sequences, predicted to result in abolished splicing; and one deep intronic variant, which has been demonstrated to completely abolish correct splicing.[18]

Investigative Ophthalmology & Visual Science

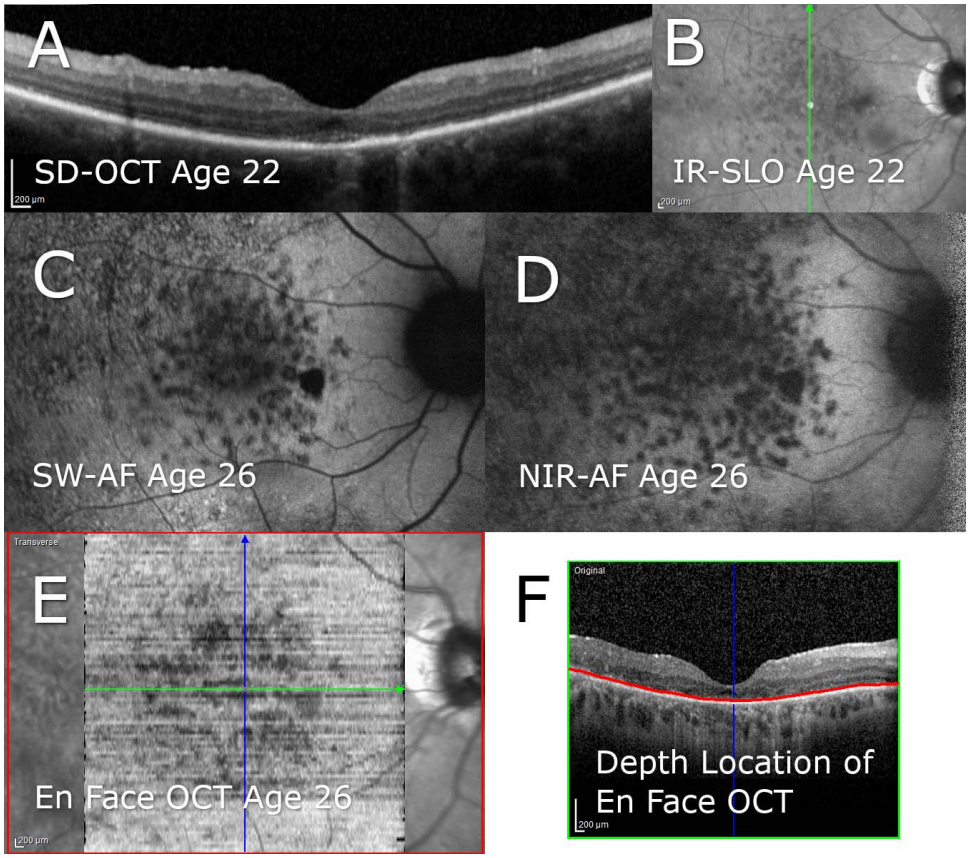

Figure 5. Multimodal imaging of AR *PROM1* patient 1. A vertical SD-OCT b-scan obtained at age 22 is shown in (**A**), with the corresponding IR-SLO image shown in (**B**). SW-AF (**C**) and NIR-AF (**D**) are overall similar, but locally more extensive changes are observable with the NIR-AF. The SW-AF shows very little focal hyperautofluorescence. The en face image in (**E**) is a mean intensity projection covering an area of 20° by 20°, at a distance of 24 µm anterior to Bruch's membrane, with a thickness of 10 µm. This depth location, at the anterior aspect of the retinal pigment epithelium, is demarcated by a *red band* on a horizontal SD-OCT b-scan in (**F**). The en face image (**E**) showed hyporeflective foci, which largely corresponded to the patterns of hypoautofluorescence in (**C**) and (**D**).

Three of the six variants were previously reported,[15–18] and the remaining three variants are new (Table 1). This study also underscores an importance of resorting to WGS in some cases in which the causal variants are not discovered by WES, but in which phenotype guides the genetic screening, and deep intronic variants (point mutations or large copy number variants) are expected to occur.

The horizontally oval macular lesions found in our patients can be seen in several previously published cases with color photography and SW-AF imaging, in patients whose ages varied from 17 to 27 years.[2–4,6] Pras et al.[2] described these oval macular lesions as a "peri-foveal ring of RPE hypertrophy bordered centrally and peripherally with RPE atrophy."

The NIR-AF findings of small, circular areas of hypo-AF were notable in that the lesions were not readily apparent on fundoscopy or color photography. The autofluorescent pigment imaged with NIR-AF is believed to be melanin,[19] and the small hypo-AF lesions likely represent focal RPE atrophy. Reinforcing this assumption is our finding of hyporeflective foci corresponding to the hypo-AF lesions at the anterior aspect of the RPE on en face OCT imaging (Fig. 5E). Two AR *PROM1* cases from previous studies have shown focal hypo-AF that were concentrated more in the arcades than in the macula and less prominently circular.[3,6] In a third case, a 19-year-old, fluorescein angiography was performed, demonstrating a cluster of hyperfluorescent circular lesions in the macula that were of a very similar size and distribution to the hypo-AF lesions of patient 1 in the present study.[2] NIR-AF in patient 1 showed some hypo-AF lesions that were not present on the corresponding SW-AF (Figs. 5C, 5D). This finding is consistent with reports on *ABCA4*-associated retinopathy and age-related macular degeneration, which have demonstrated that NIR-AF tends to show changes earlier and to a greater extent than SW-AF.[19,20]

Larger circular lesions were found in the mid-periphery of three of the *PROM1*-associated arCRD cases in this report, all of whom were in their third decade of life. These circular atrophic lesions are most reminiscent of pavingstone (or cobblestone) degeneration, which is a common, benign finding that is associated with myopia and is more often seen in older adults.[21,22] As pavingstone degeneration is uncommon in young adults, the circular peripheral RPE changes in our AR *PROM1* patients are likely related to the underlying retinal degeneration.

At issue is whether and to what extent the findings described in this study are specific to AR *PROM1*. One genetic type of retinal dystrophy caused by the *CDHR1* gene shares several phenotypic similarities to AR *PROM1*. The proteins coded for by *PROM1* and *CDHR1* (also known as *PCDH21*) strongly interact, colocalizing to the base of the photoreceptor outer segments and playing interrelated roles in outer segment morphogenesis.[9] As in *PROM1*, *CDHR1* may be diagnosed as either cone-rod dystrophy or RP with prominent macular involvement.[23] Round lesions in the mid-periphery were present in at least a quarter of reported *CDHR1* cases.[24,25] A phenotype very similar to the small hypo-AF dots seen in this study can be found in at least some cases of *CDHR1* retinal

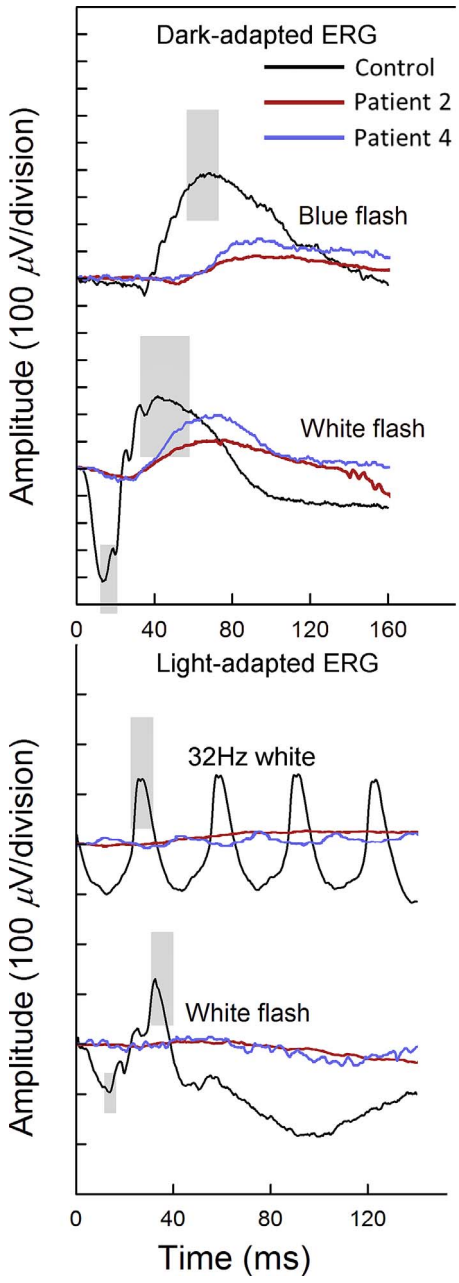

Figure 6. Full-field ERGs of AR *PROM1* patient 2 (age 15) and patient 4 (age 21). The *top panel* shows the dark-adapted responses, with the rod-isolated blue stimulus above and the combined response stimulus below. The *bottom panel* shows light-adapted responses, with the 32-Hz stimulus above, and the single-flash white stimulus below. *Gray areas* represent normative ranges for a- and b-wave amplitudes and implicit times. A control subject ERG is shown in *black*, whereas the two AR *PROM1* patients are shown in *red* (patient 2) and *blue* (patient 4).

dystrophy as well.[23,26] Review of published cases in which autofluorescence (primarily SW-AF) was performed in other genetic forms of CRD (neither *PROM1* nor *CDHR1*) showed that, with this imaging modality, a substantial majority did not resemble the cases presented here.[12,26–33] However, isolated cases of CRD associated with *C8orf37*, *CERKL*, *GUCA1A*, and *RDS* mutations did show moderate resemblances to the AF images presented here.[34–37]

The ERG phenotype discussed in this study can be found in three cases published by Eidinger et al.,[4] the youngest of whom was 8 years old at the time of testing. One AR *PROM1* patient who did not fit this ERG phenotype was a 25-year-old published by Pras et al.,[2] in whom the combined response a-wave was relatively prominent, and therefore the b/a ratio appeared to be normal. AR *PROM1* full-field ERGs have been reported to be nondetectable in most cases by the third decade of life,[1,3,5–7] setting an upper age limit to the utility of these ERG findings.

There are similarities between AR *PROM1* and *CDHR1* phenotypes on full-field ERG. Many *CDRH1* ERGs are non-detectable by the third or fourth decade.[38–40] Of the few well-described, detectable full-field ERGs that have been published, most shared the features described in this report, including a dark-adapted combined/maximal response that has an a-wave that is substantially reduced in proportion to the b-wave.[26,41,42] It might be predicted that marked cone dysfunction in conjunction with a loss of rod sensitivity would produce this ERG phenotype in diffuse photoreceptor degenerations (CRD and RP)[43,44]; however, a review of the literature for ERG waveforms in at least 16 genetic forms of nonsyndromic CRD did not find this proportionally small a-wave to be present in a notable majority of published cases.[11,27,28,34,35,37,42,45–54] Among the reviewed CRD cases, only a single *CNGA3*-associated CRD and six related individuals with *RDH12*-associated CRD were reported to have proportionally small a-waves with a dark-adapted combined response stimulus.[15,55] Also, two cases of *CNGB3*-associated achromatopsia with "impaired rod-mediated function" demonstrated a "selective a-wave reduction."[56] Thus, the proportionally reduced a-wave finding alone is not specific to AR *PROM1* (and *CDHR1*). In a less exhaustive search of non-CRD retinal dystrophies, isolated cases of *EYS* (AR RP) and *RP1* (AD RP), and two cases of AR *GUCY2D* "congenital night blindness" also demonstrated proportionally small a-waves to combined/maximal response stimuli.[57–59] These RP and congenital night blindness cases,[15,55] however, do not demonstrate the grossly delayed waveforms seen in some types of CRD, as in those from this study, or in the above-cited studies on CRD associated with *PROM1*, *CDHR1*, or *CNGA3*.[4,26,55] One more example in which the b/a ratio could be increased is *KCNV2* retinopathy, in which the a-wave tends to be approximately at the lower limit of normal, whereas the scotopic b-wave tends to be in the upper range of normal or even "super-normal."[60] Such findings would not likely be confused with *PROM1*-asoociated CRD.

The markedly reduced a-wave in combination with the delayed b-wave is likely due to the loss of cone contribution to the mixed rod-cone response in combination with substantially reduced rod pathway sensitivity. However, when a similar relative preservation of the b-wave (or relative reduction of the a-wave) was found in a rat model of *RHO*-ADRP, it was suggested that a more active process could be responsible for this finding, such as the development of ectopic rod to bipolar cell synapses in the degenerating retina.[56,61] Two studies of *Prom1* knockout mice have included a dark-adapted ERG intensity series. In both studies, the a-wave was relatively reduced to the highest luminance scotopic flashes, similar to the *RHO*-ADRP rat.[62,63]

High myopia and nystagmus have been reported to occur in AR *PROM1*, but are not pathognomonic.[3] The imaging and electrophysiological findings presented here are also not pathognomonic, and they are not evident at all ages. These findings represent observations that may aid in genotyping, either in targeted genetic testing of the *PROM1/CDHR1* genes, or in interpretation of broader genetic screens.

Patient Consent

Written consent to publish this article was obtained from the study subjects. Written informed consent was obtained under both Western IRB and the IRB of Columbia University.

Investigative Ophthalmology & Visual Science

Acknowledgments

The authors thank Carolyn Cai for expert technical assistance.

Supported by The Pangere Family Foundation; grants from the National Eye Institute/NIH EY028203, EY019007 (Core Support for Vision Research), and P30EY001792 (core grant); unrestricted funds from Research to Prevent Blindness (New York, NY, USA) to the Department of Ophthalmology, Columbia University, and the Department of Ophthalmology and Visual Sciences, University of Illinois at Chicago; and a Dolly Green Scholar award (JM) from Research to Prevent Blindness.

Disclosure: **F.T. Collison**, None; **G.A. Fishman**, None; **T. Nagasaki**, None; **J. Zernant**, None; **J.J. McAnany**, None; **J.C. Park**, None; **R. Allikmets**, None

References

1. Maw MA, Corbeil D, Koch J, et al. A frameshift mutation in prominin (mouse)-like 1 causes human retinal degeneration. *Hum Mol Genet*. 2000;9:27–34.
2. Pras E, Abu A, Rotenstreich Y, et al. Cone-rod dystrophy and a frameshift mutation in the PROM1 gene. *Mol Vis*. 2009;15:1709–1716.
3. Khan AO, Bolz HJ. Pediatric cone-rod dystrophy with high myopia and nystagmus suggests recessive PROM1 mutations. *Ophthalmic Genet*. 2015;36:349–352.
4. Eidinger O, Leibu R, Newman H, Rizel L, Perlman I, Ben-Yosef T. An intronic deletion in the PROM1 gene leads to autosomal recessive cone-rod dystrophy. *Mol Vis*. 2015;21:1295–1306.
5. Zhang Q, Zulfiqar F, Xiao X, et al. Severe retinitis pigmentosa mapped to 4p15 and associated with a novel mutation in the PROM1 gene. *Hum Genet*. 2007;122:293–299.
6. Permanyer J, Navarro R, Friedman J, et al. Autosomal recessive retinitis pigmentosa with early macular affectation caused by premature truncation in PROM1. *Invest Ophthalmol Vis Sci*. 2010;51:2656–2663.
7. Littink KW, Koenekoop RK, van den Born LI, et al. Homozygosity mapping in patients with cone–rod dystrophy: novel mutations and clinical characterizations. *Invest Ophthalmol Vis Sci*. 2010;51:5943–5951.
8. Goldberg AFX, Moritz OL, Williams DS. Molecular basis for photoreceptor outer segment architecture. *Prog Retin Eye Res*. 2016;55:52–81.
9. Yang Z, Chen Y, Lillo C, et al. Mutant prominin 1 found in patients with macular degeneration disrupts photoreceptor disk morphogenesis in mice. *J Clin Invest*. 2008;118:2908–2916.
10. Michaelides M, Gaillard M-C, Escher P, et al. The PROM1 Mutation p.R373C causes an autosomal dominant bull's eye maculopathy associated with rod, rod–cone, and macular dystrophy. *Invest Ophthalmol Vis Sci*. 2010;51:4771–4780.
11. Boulanger-Scemama E, El Shamieh S, Démontant V, et al. Next-generation sequencing applied to a large French cone and cone-rod dystrophy cohort: mutation spectrum and new genotype-phenotype correlation. *Orphanet J Rare Dis*. 2015;10:85.
12. Birtel J, Eisenberger T, Gliem M, et al. Clinical and genetic characteristics of 251 consecutive patients with macular and cone/cone-rod dystrophy. *Sci Rep*. 2018;8:4824.
13. Peachey NS, Fishman GA, Derlacki DJ, Alexander KR. Rod and cone dysfunction in carriers of X-linked retinitis pigmentosa. *Ophthalmology*. 1988;95:677–685.
14. Barnes CS, Alexander KR, Fishman GA. A distinctive form of congenital stationary night blindness with cone ON-pathway dysfunction. *Ophthalmology*. 2002;109:575–583.
15. Beryozkin A, Zelinger L, Bandah-Rozenfeld D, et al. Identification of mutations causing inherited retinal degenerations in the Israeli and Palestinian populations using homozygosity mapping. *Invest Ophthalmol Vis Sci*. 2014;55:1149–1160.
16. Song J, Smaoui N, Ayyagari R, et al. High-throughput retina-array for screening 93 genes involved in inherited retinal dystrophy. *Invest Ophthalmol Vis Sci*. 2011;52:9053–9060.
17. Carss KJ, Arno G, Erwood M, et al. Comprehensive rare variant analysis via whole-genome sequencing to determine the molecular pathology of inherited retinal disease. *Am J Hum Genet*. 2017;100:75–90.
18. Mayer AK, Rohrschneider K, Strom TM, et al. Homozygosity mapping and whole-genome sequencing reveals a deep intronic *PROM1* mutation causing cone–rod dystrophy by pseudoexon activation. *Eur J Hum Genet*. 2016;24:459.
19. Kellner S, Kellner U, Weber BHF, Fiebig B, Weinitz S, Ruether K. Lipofuscin- and melanin-related fundus autofluorescence in patients with ABCA4-associated retinal dystrophies. *Am J Ophthalmol*. 2009;147:895–902.e1.
20. Kellner U, Kellner S, Weinitz S. Fundus autofluorescence (488 NM) and near-infrared autofluorescence (787 NM) visualize different retinal pigment epithelium alterations in patients with age-related macular degeneration. *Retina*. 2010;30:6–15.
21. Karlin DB, Curtin BJ. Peripheral chorioretinal lesions and axial length of the myopic eye. *Am J Ophthalmol*. 1976;81:625–635.
22. Pierro L, Camesasca FI, Mischi M, Brancato R. Peripheral retinal changes and axial myopia. *Retina*. 1992;12:12–17.
23. Riera M, Navarro R, Ruiz-Nogales S, et al. Whole exome sequencing using Ion Proton system enables reliable genetic diagnosis of inherited retinal dystrophies. *Sci Rep*. 2017;7:42078.
24. Henderson RH, Li Z, El Aziz MMA, et al. Biallelic mutation of Protocadherin-21 (PCDH21) causes retinal degeneration in humans. *Mol Vis*. 2010;16:46–52.
25. Bessette AP, DeBenedictis MJ, Traboulsi EI. Clinical characteristics of recessive retinal degeneration due to mutations in the CDHR1 gene and a review of the literature. *Ophthalmic Genet*. 2018;39:51–55.
26. Ba-Abbad R, Sergouniotis PI, Plagnol V, et al. Clinical characteristics of early retinal disease due to CDHR1 mutation. *Mol Vis*. 2013;19:2250–2259.
27. Robson AG, Michaelides M, Saihan Z, et al. Functional characteristics of patients with retinal dystrophy that manifest abnormal parafoveal annuli of high density fundus autofluorescence; a review and update. *Doc Ophthalmol*. 2008;116:79–89.
28. Ebenezer ND, Michaelides M, Jenkins SA, et al. Identification of novel RPGR ORF15 mutations in X-linked progressive cone-rod dystrophy (XLCORD) families. *Invest Ophthalmol Vis Sci*. 2005;46:1891–1898.
29. Matsui R, McGuigan DB III, Gruzensky ML, et al. SPATA7: Evolving phenotype from cone-rod dystrophy to retinitis pigmentosa. *Ophthalmic Genet*. 2016;37:333–338.
30. Fakin A, Robson AG, Fujinami K, et al. Phenotype and progression of retinal degeneration associated with nullizigosity of ABCA4. *Invest Ophthalmol Vis Sci*. 2016;57:4668–4678.
31. Zobor D, Zrenner E, Wissinger B, Kohl S, Jägle H. GUCY2D- or GUCA1A-related autosomal dominant cone-rod dystrophy: is there a phenotypic difference? *Retina*. 2014;34:1576–1587.
32. Paunescu K, Preising MN, Janke B, Wissinger B, Lorenz B. Genotype-phenotype correlation in a German family with a novel complex CRX mutation extending the open reading frame. *Ophthalmology*. 2007;114:1348–1357.e1.
33. Michaelides M, Holder GE, Hunt DM, Fitzke FW, Bird AC, Moore AT. A detailed study of the phenotype of an autosomal dominant cone-rod dystrophy (CORD7) associated with mutation in the gene for RIM1. *Br J Ophthalmol*. 2005;89:198–206.

34. Nong E, Lee W, Merriam JE, Allikmets R, Tsang SH. Disease progression in autosomal dominant cone-rod dystrophy caused by a novel mutation (D100G) in the GUCA1A gene. *Doc Ophthalmol*. 2014;128:59–67.
35. van Huet RAC, Estrada-Cuzcano A, Banin E, et al. Clinical characteristics of rod and cone photoreceptor dystrophies in patients with mutations in the C8orf37 gene. *Invest Ophthalmol Vis Sci*. 2013;54:4683–4690.
36. Duncan JL, Talcott KE, Ratnam K, et al. Cone structure in retinal degeneration associated with mutations in the peripherin/RDS gene. *Invest Ophthalmol Vis Sci*. 2011;52:1557–1566.
37. Aleman TS, Soumittra N, Cideciyan AV, et al. CERKL mutations cause an autosomal recessive cone-rod dystrophy with inner retinopathy. *Invest Ophthalmol Vis Sci*. 2009;50:5944–5954.
38. Duncan JL, Roorda A, Navani M, et al. Identification of a novel mutation in the CDHR1 gene in a family with recessive retinal degeneration. *Arch Ophthalmol*. 2012;130:1301–1308.
39. Nikopoulos K, Avila-Fernandez A, Corton M, et al. Identification of two novel mutations in CDHR1 in consanguineous Spanish families with autosomal recessive retinal dystrophy. *Sci Rep*. 2015;5:13902.
40. Ostergaard E, Batbayli M, Duno M, Vilhelmsen K, Rosenberg T. Mutations in PCDH21 cause autosomal recessive cone-rod dystrophy. *J Med Genet*. 2010;47:665–669.
41. Cohen B, Chervinsky E, Jabaly-Habib H, Shalev SA, Briscoe D, Ben-Yosef T. A novel splice site mutation of CDHR1 in a consanguineous Israeli Christian Arab family segregating autosomal recessive cone-rod dystrophy. *Mol Vis*. 2012;18:2915–2921.
42. Lazar CH, Mutsuddi M, Kimchi A, et al. Whole exome sequencing reveals GUCY2D as a major gene associated with cone and cone-rod dystrophy in Israel. *Invest Ophthalmol Vis Sci*. 2014;56:420–430.
43. Berson EL. Retinitis pigmentosa. The Friedenwald Lecture. *Invest Ophthalmol Vis Sci*. 1993;34:1659–1676.
44. Birch DG, Fish GE. Rod ERGs in retinitis pigmentosa and cone-rod degeneration. *Invest Ophthalmol Vis Sci*. 1987;28:140–150.
45. Birch DG, Peters AY, Locke KL, Spencer R, Megarity CF, Travis GH. Visual function in patients with cone–rod dystrophy (CRD) associated with mutations in the ABCA4 (ABCR) gene. *Exp Eye Res*. 2001;73:877–886.
46. Fishman GA, Stone EM, Eliason DA, Taylor CM, Lindeman M, Derlacki DJ. ABCA4 gene sequence variations in patients with autosomal recessive cone-rod dystrophy. *Arch Ophthalmol*. 2003;121:851–855.
47. Al Sulaiman H, Schatz P, Nowilaty SR, Abdelkader E, Abu Safieh L. Diffuse retinal vascular leakage and cone-rod dystrophy in a family with the homozygous missense c.1429G>A (p.Gly477Arg) mutation in CRB1 [published online ahead of print December 1, 2017]. *Retin Cases Brief Rep*. doi:10.1097/ICB.0000000000000654.
48. Xu F, Dong F, Li H, Li X, Jiang R, Sui R. Phenotypic characterization of a Chinese family with autosomal dominant cone-rod dystrophy related to GUCY2D. *Doc Ophthalmol*. 2013;126:233–240.
49. Kitiratschky VBD, Nagy D, Zabel T, et al. Cone and cone-rod dystrophy segregating in the same pedigree due to the same novel CRX gene mutation. *Br J Ophthalmol*. 2008;92:1086–1091.
50. Michaelides M, Holder GE, Webster AR, et al. A detailed phenotypic study of "cone dystrophy with supernormal rod ERG." *Br J Ophthalmol*. 2005;89:332–339.
51. Lines MA, Hébert M, McTaggart KE, Flynn SJ, Tennant MT, MacDonald IM. Electrophysiologic and phenotypic features of an autosomal cone-rod dystrophy caused by a novel CRX mutation. *Ophthalmology*. 2002;109:1862–1870.
52. Kjellström U. Association between genotype and phenotype in families with mutations in the ABCA4 gene. *Mol Vis*. 2014;20:89–104.
53. Simonelli F, Testa F, Zernant J, et al. Association of a homozygous nonsense mutation in the ABCA4 (ABCR) gene with cone-rod dystrophy phenotype in an Italian family. *Ophthalmic Res*. 2004;36:82–88.
54. Zou X, Fu Q, Fang S, et al. Phenotypic variability of recessive RDH12-associated retinal dystrophy [published online ahead of print August 21, 2018]. *Retina*. doi:10.1097/IAE.0000000000002242.
55. Shaikh RS, Reuter P, Sisk RA, et al. Homozygous missense variant in the human CNGA3 channel causes cone-rod dystrophy. *Eur J Hum Genet*. 2015;23:473–480.
56. Khan NW, Wissinger B, Kohl S, Sieving PA. CNGB3 achromatopsia with progressive loss of residual cone function and impaired rod-mediated function. *Invest Ophthalmol Vis Sci*. 2007;48:3864–3871.
57. Collin RWJ, Littink KW, Klevering BJ, et al. Identification of a 2 Mb human ortholog of *Drosophila* eyes shut/spacemaker that is mutated in patients with retinitis pigmentosa. *Am J Hum Genet*. 2008;83:594–603.
58. Gamundi MJ, Hernan I, Martínez-Gimeno M, et al. Three novel and the common Arg677Ter RP1 protein truncating mutations causing autosomal dominant retinitis pigmentosa in a Spanish population. *BMC Med Genet*. 2006;7:35.
59. Stunkel ML, Brodie SE, Cideciyan AV, et al. Expanded retinal disease spectrum associated with autosomal recessive mutations in GUCY2D. *Am J Ophthalmol*. 2018;190:58–68.
60. Collison FT, Park JC, Fishman GA, Stone EM, McAnany JJ. Two-color pupillometry in KCNV2 retinopathy [published online ahead of print March 29, 2019]. *Doc Ophthalmol*. doi:10.1007/s10633-019-09691-w.
61. Aleman TS, LaVail MM, Montemayor R, et al. Augmented rod bipolar cell function in partial receptor loss: an ERG study in P23H rhodopsin transgenic and aging normal rats. *Vision Res*. 2001;41:2779–2797.
62. Zacchigna S, Oh H, Wilsch-Bräuninger M, et al. Loss of the cholesterol-binding protein prominin-1/CD133 causes disk dysmorphogenesis and photoreceptor degeneration. *J Neurosci*. 2009;29:2297–2308.
63. Dellett M, Sasai N, Nishide K, et al. Genetic background and light-dependent progression of photoreceptor cell degeneration in Prominin-1 knockout mice. *Invest Ophthalmol Vis Sci*. 2014;56:164–176.

Investigative Ophthalmology & Visual Science